Reaction Mechanism of Porphyrin Metallation Studied by Theoretical Methods

Yong Shen[a, b] and Ulf Ryde*[a]

Abstract: We have studied the reaction mechanism for the insertion of Mg^{2+} and Fe^{2+} into a porphyrin ring with density functional calculations with large basis set and including solvation, zero-point and thermal effects. We have followed the reaction from the outer-sphere complex, in which the metal is coordinated with six water molecules and the porphyrin is doubly protonated, until the metal ion is inserted into the deprotonated porphyrin ring with only one water ligand remaining. This reaction involves the stepwise displacement of five water molecules and the removal of two protons from the porphyrin ring. In addition, a step seems to be necessary in which a porphyrin pyrrolenine nitrogen atom changes its interaction from a hydrogen bond to a metal-bound solvent molecule to a direct coordination to the metal ion. If the protons are taken up by a neutral imidazole molecule, the deprotonation reactions are exothermic with minimal barriers. However, with a water molecule as an acceptor, they are endothermic. The ligand exchange reactions were approximately thermoneutral (± 20 kJ mol^{-1}, with one exception) with barriers of up to 72 kJ mol^{-1} for Mg and 51 kJ mol^{-1} for Fe. For Mg, the highest barrier was found for the formation of the first bond to the porphyrin ring. For Fe, a higher barrier was found for the formation of the second bond to the porphyrin ring, but this barrier is probably lower in solution. No evidence was found for an initial pre-equilibrium between a planar and a distorted porphyrin ring. Instead, the porphyrin becomes more and more distorted as the number of metal–porphyrin bonds increase (by up to 191 kJ mol^{-1}). This strain is released when the porphyrin becomes deprotonated and the metal moves into the ring plane. Implications of these findings for the chelatase enzymes are discussed.

Keywords: density functional calculations · iron · magnesium · metalation · porhyrinoids

Introduction

Metal complexes of tetrapyrroles are common in biological systems, for example, haem, chlorophyll, vitamin B_{12} and coenzyme F430. Together, they provide essential cofactors for a huge number of enzymes. Therefore, they have attracted much interest from all parts of chemistry.[1] These cofactors are synthesised in the organism in a complicated sequence of reactions. One step in this sequence is the insertion of the metal ion into the tetrapyrrole ring system. This step has been extensively studied both in solution[2,3] and in biological systems, in which the reaction is catalysed by so-called chelatases.[4–9]

In particular, the metallation of a porphyrin molecule has been studied by many groups.[10–14] The consensus seems to be that the reaction mechanism in solution consists of the following steps: deformation of the porphyrin ring, outer-sphere association of the solvated metal ion and the porphyrin, exchange of a solvent molecule with the first pyrrolenine nitrogen atom, chelate-ring closure with the expulsion of more solvent molecules, first deprotonation of a pyrrole nitrogen atom and finally deprotonation of the second nitrogen atom, which leads to the formation of the metalloporphyrin (some authors prefer to switch the first two steps).

The rate by which metal ions are inserted into the porphyrin ring typically follows the order Cu > Zn > Mn, Co, Fe > Ni > Cd ≫ Mg.[3,11] For most metals, the formation of the first bond to the porphyrin ring seems to be rate limiting.[10,11,13,14] Thus, the metallation reaction is similar to a normal solvent-exchange reaction, although the rate is 5–11 orders of magnitude slower.[14] This slowing is normally at-

[a] Dr. Y. Shen, Prof. U. Ryde
Department of Theoretical Chemistry, Lund University
Chemical Centre, P. O. Box 124, 221 00 Lund (Sweden)
Fax: (+46) 46-2224543
E-mail: Ulf.Ryde@teokem.lu.se

[b] Dr. Y. Shen
School of Chemistry and Chemical Engineering
Sun Yat-Sen University, 510275, Guangzhou (P. R. China)

 DOI: 10.1002/chem.200400298

tributed to the distortion of the porphyrin ring needed to form the first bonds to the metal. Thus, porphyrins that are distorted already in the free-base form (e.g., by bulky side-chains or substituents on the pyrrole nitrogen atoms) have a 10^3–10^5 higher rate of metallation.[15]

Solvent-exchange reactions have been extensively studied also by theoretical methods, especially water exchange.[16–19] However, the metallation of porphyrins does not seem to have been studied before, even if many theoretical investigations have been published for haem, chlorophyll, vitamin B_{12}, coenzyme F430, Mg porphyrin and even for ferrochelatase.[20–33]

The intermediate formed after the chelate ring closure is often called a *sitting-atop complex* (SAT).[34] This complex has been much discussed.[35–40] Recently, sitting-atop complexes of Cu^{2+} with various porphyrins in acetonitrile have been characterised by kinetic measurements, extended X-ray absorption fine structure (EXAFS) and nuclear magnetic resonance (NMR) methods.[10,41,42] The complex was suggested to be six-coordinate with three kinds of Cu–N interactions with bond lengths of 205, 198 and 232 pm for pyrrolenine nitrogen atoms of the porphyrin and for acetonitrile nitrogen atoms at equatorial and axial sites, respectively.[10] We have performed a density functional study of possible SAT complexes between porphyrin and Mg^{2+}, Fe^{2+} or Cu^{2+}.[43] We showed that there are numerous possible structures with 1–5 solvent molecules, one or two metal ions and *cis* or *trans* protonation of the porphyrin ring. Many of these have similar energies and their relative stabilities vary with the metal ion. Therefore, the interpretation of the EXAFS data is far from straightforward.[38,43]

In this paper, we use these data to study the detailed mechanism of the metallation reaction of porphyrin rings with Mg^{2+} and Fe^{2+}. We have characterised all transition-state structures on the pathway from the outer-sphere complex to metallated porphyrin (i.e., complexes involving 1–6 water molecules). For each step, we calculated the reaction and activation energies, including solvation, zero-point and thermal effects. We also studied the deprotonation of the pyrrole nitrogen atoms in the SAT by imidazole or water molecule in two subsequent steps. Together, these results give an important insight in the metallation reaction and indicate that the consensus reaction mechanism has to be modified in a some aspects. They also give some clues to the corresponding biological reaction in the chelatase enzymes.

Results and Discussion

In the following, we will first describe the results for the metallation of a porphyrin ring by Mg^{2+} in a rather detailed way. Then, the corresponding results for Fe^{2+} will be briefly described, emphasizing differences between Fe^{2+} and Mg^{2+}. Finally, we will discuss the effect of including an extra water molecule, hydrogen bonded to the porphyrin pyrrole hydrogen atoms on the opposite side of the ring, and the metallation of a methylated porphyrin ring.

Formation of the first Mg–N_{Pyrn} bond: As mentioned in the introduction, the three first steps in the metallation of porphyrin are usually suggested to be deformation of the porphyrin ring, outer-sphere association of the solvated metal ion and the (protonated) porphyrin, and exchange of a solvent molecule with the first pyrrolenine nitrogen atom (N_{Pyrn}, i.e., an unprotonated porphyrin nitrogen atom).[10–14] The formation of the outer-sphere complex is usually assumed to be diffusion controlled.[10,11] This reaction is hard to study by quantum chemical methods. Therefore, we have only optimised the structure of the outer-sphere complex, which is shown in Figure 1. It is 92 kJ mol^{-1} less stable than isolated $Mg(H_2O)_6$ and $PorH_2$; however, this energy is very uncertain, because it involves extensive energy corrections of differing signs from solvation, thermal effect and the method (all reported energies in the text are ΔG values, including solvation effects; the individual terms are presented in the tables). As can be seen in Table 1, the Mg–O distances in the outer-sphere complex are 204–213 pm, compared to 210 pm in the free $Mg(H_2O)_6$ complex. The Mg–N distances are 390–508 pm. The strain energy of the porphyrin ring is 28 kJ mol^{-1} (i.e., the energy of $PorH_2$ in this complex compared to that in its optimised vacuum geometry; Table 2).

Figure 1. The first reaction of $Mg(H_2O)_6$ with $PorH_2$, 6+0 to 5+1,1N.

It has earlier been suggested that there should be a rapid equilibrium between a planar and a distorted porphyrin, in which the pyrrolenine nitrogen atoms become more exposed to the solvent. This equilibrium should then provide the first step of the metallation reaction. If this was the case, there should be a distorted structure as a local minimum on the potential-energy surface of the porphyrin molecule. For our porphyrin model, we have not been able to find such a structure. Instead, the ring system distorts successively as the Mg–N bonds are formed. Thus, in our view, the distortion of the porphyrin ring is a part of all steps in the metallation reaction, not a separate, initial step. However, it should be noted that if explicit water molecules are included in the calculations (on the side opposite to Mg), the porphyrin ring becomes significantly distorted, owing to hydro-

Table 1. Mg–ligand distances [pm] in the studied Mg complexes.

Complex	$Mg–N_{Pyrn}$	$Mg–N_{Pyr}$	Mg–O	$N_{Pyr}–H$	$N_{Im}–H$
6+0	449.3, 414.5	390.1, 508.0	204.1, 210.5, 210.8, 211.1, 211.2, 213.4		
ts65	332.1, 447.9	403.5, 413.0	206.4, 208.3, 209.5, 211.8, 212.1, 248.9		
5+1,1N	232.0, 432.1	365.4, 368.2	205.8, 210.1, 212.5, 213.0, 213.7, 377.7		
5+0,1N	230.5, 429.4	360.3, 368.2	205.8, 211.3, 211.9, 213.1, 214.5		
ts54	218.7, 415.0	341.3, 355.4	205.1, 209.3, 209.8, 210.9, 280.8		
4+1,1N	216.0, 414.9	343.4, 345.3	202.6, 204.3, 207.5, 213.8, 390.7		
4+0,1N	214.0, 408.9	338.2, 341.0	203.3, 206.7, 207.4, 214.6		
ts4	227.2, 300.1	259.2, 308.5	214.8, 216.0, 217.2, 220.2		
4+0	242.8, 246.8	266.6, 267.5	223.2, 223.5, 223.7, 223.8		
4+0	242.8, 246.8	266.6, 267.5	223.2, 223.5, 223.7, 223.8		
ts432	239.4, 240.5	269.6, 252.9	216.7, 218.0, 228.2, 254.2		
3+1	232.6, 235.6	233.5, 283.1	208.7, 214.4, 220.4, 412.7		
4+0,1N	214.0, 408.9	338.2, 341.0	203.3, 206.7, 207.4, 214.6		
ts431	211.5, 396.3	326.5, 331.4	197.3, 202.8, 203.3, 271.7		
3+1,1N	210.2, 390.5	314.6, 331.7	194.0, 203.3, 203.4, 377.3		
3+0,1N	210.4, 361.2	249.6, 338.4	197.4, 204.9, 208.8		
ts3	216.8, 286.9	234.8, 288.1	207.2, 210.7, 211.5		
3+0	232.0, 233.0	230.8, 281.3	212.7, 215.7, 219.0		
3+0	232.0, 233.0	230.8, 281.3	212.7, 215.7, 219.0		
ts32	224.5, 228.4	234.9, 254.9	210.8, 213.9, 272.2		
2+1	222.5, 222.7	241.5, 243.9	208.8, 210.2, 421.4		
2+0	221.9, 221.9	236.7, 237.8	211.7, 212.9		
ts21	216.4, 218.2	230.9, 232.9	204.4, 272.0		
1+1	214.7, 215.2	228.2, 228.4	199.7, 413.4		
6+0 + $PorH_2$ + H_2O	408.6, 438.1	392.8, 493.3	203.7, 210.6, 210.7, 211.5, 212.0, 213.4		
ts65 + $PorH_2$ + H_2O	334.4, 445.9	407.2, 409.1	206.1, 207.8, 210.1, 211.7, 212.6, 247.0		
5+1,1N + $PorH_2$ + H_2O	228.6, 428.8	354.4, 368.7	203.3, 214.0, 214.6, 214.9, 215.1, 375.0		
6+0 $PorHCH_3$	435.9, 482.3	407.8, 450.0	201.9, 209.2, 211.2, 211.7, 211.8, 211.9		
ts65 $PorHCH_3$	333.1, 450.1	400.9, 440.8	205.0, 208.8, 210.0, 212.7, 212.8, 246.4		
5+1,1N $PorHCH_3$	230.4, 433.4	367.5, 384.5	203.2, 212.7, 213.7, 214.2, 214.6, 377.1		
3+0,1N $PorHCH_3$	208.6, 360.6	252.8, 344.6	195.3, 205.6, 209.2		
ts3 $PorHCH_3$	210.9, 306.0	241.8, 289.8	204.0, 210.4, 211.2		
3+0,2N $PorHCH_3$	228.6, 228.6	231.7, 277.0	215.0, 220.1, 222.2		
	$Mg–N_{Pyrn}$	$Mg–N_{Pyr}$	Mg–O	$N_{Pyr}–H$	$N_{Im}–H$
[$(H_2O)_2$MgPorH$_2$] + Im	218.6, 218.8	237.3, 237.5	214.2, 214.5	105.8, 105.8	196.5, 196.8
tsH2Im	219.9, 220.4	227.1, 242.6	213.5, 215.0	103.3, 116.9	150.8, 297.7
[$(H_2O)_2$MgPorH] + ImH	219.4, 221.0	214.4, 246.9	213.1, 218.6	102.8, 187.0	105.8, 371.8
[$(H_2O)_2$MgPorH] + Im	214.5, 216.9	213.0, 234.5	216.7, 232.6	110.5	165.0
tsHIm	215.6, 217.0	215.5, 230.2	217.6, 229.2	127.8	132.6
[$(H_2O)_2$MgPor] + ImH	215.7, 217.7	216.2, 223.7	219.2, 228.6	165.5	109.5
	$Mg–N_{Pyrn}$	$Mg–N_{Pyr}$	Mg–O	$N_{Pyr}–H$	$O_{Wat}–H$
[$(H_2O)_2$MgPorH$_2$] + H_2O	221.2, 221.2	236.8, 237.0	212.9, 213.1	104.9, 104.9	191.7, 191.9
[$(H_2O)_2$MgPorH] + H_3O	218.2, 230.7	220.7, 246.6	210.6, 216.3	103.0, 149.3	105.0, 264.9
[$(H_2O)_2$MgPorH] + H_2O	211.7, 217.9	220.2, 241.7	215.4, 222.0	107.4	166.9
[$(H_2O)_2$MgPor] + H_3O	216.4, 221.6	224.8, 233.1	215.0, 218.2	143.8	109.0
[(H_2O)MgPorH$_2$]	212.6, 212.7	226.0, 226.2	205.1		
[(H_2O)MgPorH$_2$] + H_2O	212.3, 212.3	224.1, 224.1	205.8, 285.1	104.8, 104.8	195.7, 195.7
[(H_2O)MgPorH] + H_3O	211.4, 216.0	218.5, 230.3	205.6	103.4, 150.6	104.8, 291.8
[(H_2O)MgPorH]	206.5, 210.1	210.1, 229.1	209.7		
[(H_2O)MgPorH] + H_2O	205.3, 225.8	208.5, 208.7	213.7, 232.2	104.1	189.6
[(H_2O)MgPor] + H_3O	210.7, 211.4	217.3, 222.5	208.2	144.3	109.2
[(H_2O)mgPor]	208.2, 208.2	210.6, 210.8	217.5		
[H_2O + (H_2O)mgPor]	209.6, 210.1	210.7, 211.6	210.5, 381.2		
[MgPor]	207.2, 207.2	207.2, 207.2			

gen bonds formed by water and the central pyrrole nitrogen atoms.[43] This will be discussed below.

Therefore, we have followed the reaction as the successive exchange of water ligands with the nitrogen atoms of the porphyrin. The resulting Mg–ligand distances are given in Table 1 and energies are compiled in Table 2. In the first step, one of the water molecules in the first coordination shell of Mg is replaced by an N_{Pyrn} atom, giving rise to the complex in Figure 1c. It has five first-sphere water molecules, one second-sphere water molecule and Mg forms one bond to the porphyrin with an $Mg–N_{Pyrn}$ distance of 232 pm. The other N_{Pyrn} atom forms a hydrogen bond to an Mg-bound water molecule. We will call this type of structure 5+1,1N in the following (indicating five first- and one second-sphere water molecules and only one bond between the metal ion and the porphyrin ring). It is 21 kJ mol^{-1} less stable than the outer-sphere complex, mainly owing to unfavourable solvation and thermal effects. The strain energy has increased by 7 kJ mol^{-1}.

The transition state between these two structures (Figure 1b) nicely represents the exchange reaction: the $Mg–N_{Pyrn}$ distance is 332 pm and the Mg–O distance of the reacting water molecules is 249 pm. It is 72 kJ mol^{-1} less stable than the outer-sphere complex and it is characterised by an imaginary frequency of 119 cm^{-1}, the eigenvector of which nicely follows the O–Mg–N reaction coordinate.

Formation of the second $Mg–N_{Pyrn}$ bond: Next, we want to form the second $Mg–N_{Pyrn}$ bond. It turned out that this is not fully straight forward, owing to the strong hydrogen

Table 2. Energies [in kJ mol^{-1}] of the optimised Mg complexes. ΔE is the relative energy at the BP86/6-31G* level. $\Delta\Delta$Method is the change in relative energy at the B3LYP/6-311+G(2d,2p) level. $\Delta\Delta$Solv and $\Delta\Delta$Thermal are the changes in the relative energy owing to solvation and thermal (zero-point, as well thermal corrections to the Gibbs free energy) effects, respectively. ΔG is the final estimate of the free energy. E_{deprot} is the deprotonation energy of the complex in solution. ΔE_{Porph} is the energy of the porphyrin ring in this complex, relative to optimised structure in vacuum. Finally, Imag f is the value of the imaginary frequency [cm^{-1}] for the transition structure.

	ΔE	$\Delta\Delta$Solv	$\Delta\Delta$Method	$\Delta\Delta$Thermal	ΔG	E_{deprot}	ΔE_{Porph}	Imag f
$Mg(H_2O)_6+PorH_2$	225.7	−214.6	−38.8	−64.9	−92.5	−1326.1	0.0	–
6+0	0.0	0.0	0.0	0.0	0.0	–	27.5	–
ts65	39.3	14.5	11.4	6.4	71.6	–	–	118.6
5+1,1N	−19.5	22.3	7.9	10.3	21.0	–	34.5	–
5+0,1N	0.0	0.0	0.0	0.0	0.0	−1240.4	35.7	–
ts54	12.5	6.0	5.6	4.4	28.4	–	–	93.7
4+1,1N	−21.8	4.2	−2.6	5.6	−14.6	–	36.3	–
4+0,1N	0.0	0.0	0.0	0.0	0.0	−1177.7	39.3	–
ts4	51.5	6.8	16.3	7.8	82.4	–	–	52.5
4+0	48.9	11.2	22.5	6.4	88.9	−1110.3	92.8	–
4+0	0.0	0.0	0.0	0.0	0.0	−1110.3	92.8	–
ts432	1.5	1.2	−0.1	1.7	4.4	–	–	94.7
3+1	−30.4	7.1	−19.3	−8.9	−51.5	–	114.5	–
4+0,1N	0.0	0.0	0.0	0.0	0.0	−1177.7	39.3	–
ts431	11.8	7.6	1.9	−1.2	20.1	–	–	112
3+1,1N	−15.5	20.0	−0.2	−9.5	−5.2	–	52.1	–
3+0,1N	0.0	0.0	0.0	0.0	0.0	−1161.9	75.5	–
ts3	14.0	1.5	3.5	10.7	29.7	–	–	92.8
3+0	4.6	0.7	2.9	8.6	16.7	−1140.0	120.1	–
3+0	0.0	0.0	0.0	0.0	0.0	−1140.0	120.1	–
ts32	7.1	4.5	1.6	6.1	19.4	–	–	112.9
2+1	−9.3	14.6	−9.6	−1.6	−5.8	–	150.4	–
2+0	0.0	0.0	0.0	0.0	0.0	−1125.7	158.1	–
ts21	9.5	4.3	2.1	3.4	19.3		–	105.6
1+1	−14.3	20.3	−5.0	1.1	2.1	–	182.7	–
1+0	–	–	–	–	–	−1097.3	195.4	–
$[(H_2O)_2MgPorH_2]+Im$	0.0	0.0	0.0	0.0	0.0	–	–	–
tsH2Im	1.8	2.3	4.3	−8.2	0.1	–	–	74.4
$[(H_2O)_2MgPorH]+ImH$	−26.6	−4.1	−7.2	−2.9	−40.8	–	–	–
$[(H_2O)_2MgPorH]+Im$	0.0	0.0	0.0	0.0	0.0	–	–	–
tsHIm	4.2	−4.2	9.0	−10.5	−1.4	–	–	773.6
$[(H_2O)_2MgPor]+ImH$	−2.4	−15.2	0.3	−0.2	−17.4	–	13.1	–
$[(H_2O)_2MgPorH_2]+H_2O$	0.0	0.0	0.0	0.0	0.0	–	–	–
$[(H_2O)_2MgPorH]+H_3O$	0.0	−13.3	11.3	−2.7	74.0	–	114.9	–
$[(H_2O)_2MgPorH]+H_2O$	0.0	0.0	0.0	0.0	0.0	–	–	–
$[(H_2O)_2MgPor]+H_3O$	0.0	4.6	19.4	4.4	70.3	–	23.3	–
$[(H_2O)MgPorH_2]+H_2O$	0.0	0.0	0.0	0.0	0.0	–	–	–
$[(H_2O)MgPorH]+H_3O$	0.0	−16.6	9.6	−1.2	75.0	–	–	–
$[(H_2O)MgPorH]+H_2O$	0.0	0.0	0.0	0.0	0.0	–	–	–
$[(H_2O)MgPor]+H_3O$	0.0	−3.8	17.4	1.1	80.0	–	–	–
$[(H_2O)MgPorH_2]+H_2O$[a]	0.0	0.0	0.0	0.0	0.0	–	–	–
$[(H_2O)MgPorH]+H_3O$[a]	0.0	67.3	18.1	−0.5	24.2	–	–	–
$[(H_2O)MgPorH]+H_2O$[a]	0.0	0.0	0.0	0.0	0.0	–	–	–
$[(H_2O)MgPor]+H_3O$[a]	0.0	−201.5	23.8	0.1	83.6	–	–	–
$H_2O+[(H_2O)MgPor]$	–	–	–	–	–	–	5.8	–
$[(H_2O)MgPor]$	–	–	–	–	–	–	7.7	–
[MgPor]	–	–	–	–	–	–	9.1	–
$6+0PorH_2+H_2O$	0.0	0.0	0.0	0.0	0.0	–	64.4	–
$ts65PorH_2+H_2O$	0.0	11.8	4.4	3.9	70.7	–	–	117.4
$5+1,1NPorH_2+H_2O$	0.0	18.9	5.4	5.7	16.0	–	69.4	–
6+0 $PorHCH_3$	0.0	0.0	0.0	0.0	0.0	–	22.9	–
ts65 $PorHCH_3$	52.1	10.3	11.3	9.6	83.2	–	–	109.1
5+1,1N $PorHCH_3$	−14.0	20.5	8.6	15.8	30.9	–	31.0	–
3+0,1N $PorHCH_3$	0.0	0.0	0.0	0.0	0.0	–	73.0	–
ts3 $PorHCH_3$	6.9	2.1	5.8	12.2	27.0	–	87.5	77.4
3+0,2N $PorHCH_3$	−16.0	2.9	5.8	16.3	9.0	–	91.3	–

[a] Separated reactants and products.

bond between an Mg-bound water molecule and the second N_{Pyrn} atom. Thus, we must remove this hydrogen bond as well as move another water molecule into the second coordination sphere. It turned out that this has to be done in separate steps.

Therefore, we started out from a complex with five first sphere water molecules (Figure 2), obtained by removing the second-sphere water molecule from the product of the previous reaction (we always removed second-sphere water molecules in this way to reduce the computational load and to minimise the problem of multiple local minima). Then, we moved one of the water molecules into the second coordination sphere, yielding the 4+1,1N complex in Figure 2c. In this complex, the Mg ion is five-coordinate and the porphyrin strain has only increased by 1 kJ mol^{-1}. It is 15 kJ mol^{-1} more stable than the 5+0,1N complex.

The transition state between these two structures is 28 kJ mol^{-1} less stable than the reactant complex. It has a Mg–O distance of 281 pm (214 pm in the reactant and 390 pm in the product complex).

Figure 2. The second reaction of Mg: 5+0,1N to 4+1,1N.

Next, we tried to find the transition from the 4+0,1N structure to the corresponding 4+0,2N structure, that is, the exchange of the N_{Pyrn}–water hydrogen bond with a Mg–N_{Pyrn} bond (Figure 3). The resulting structure has two Mg–N_{Pyrn} bonds of 243 and 247 pm. However, the formation of the second Mg–N_{Pyrn} bond increases the distortion of the porphyrin ring to 93 kJ mol^{-1}. Therefore, this structure is 89 kJ mol^{-1} less stable than the 1N complex, with rather large corrections from the basis set, solvation and thermal effects.

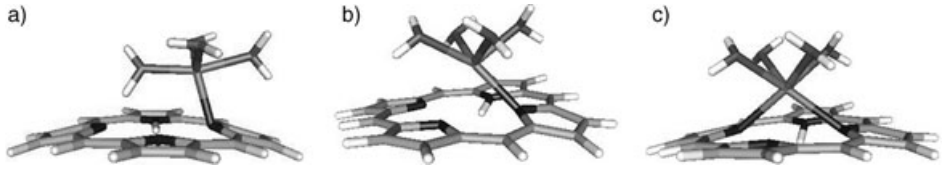

Figure 3. The third reaction of Mg: 4+0,1N to 4+0.

The corresponding transition state has slightly smaller corrections. Therefore, it is 3 kJ mol^{-1} less stable than the product without any corrections, but 7 kJ mol^{-1} more stable than the product complex (82 kJ mol^{-1} less stable than the reactant). The second Mg–N_{Pyrn} bond is 247 pm (409 pm in the reactant and 300 pm in the transition state). It is notable that all the Mg–O bonds (215–220 pm) are elongated relative to the reactant complex (203–215 pm), but appreciably shorter than in the product (223–224 pm). This elongation is caused by the quite short interactions between the two N_{Pyr} atoms (i.e., the protonated pyrrole nitrogen atoms of the porphyrin ring) and Mg (267, 259–308 and 338–341 pm in the product, transition state and the reactant, respectively). The transition state involves a rotation of the water molecules around the Fe–N_{Pyrn} axis and a partial formation of the Mg–N_{Pyrn} bond.

Formation of the third Mg–N bond: The next step in the metallation reaction is to move the third water molecule into the second coordination sphere, which also will lead to the formation of a third Mg–N bond. This reaction (4+0→3+1, Figure 4) is quite straightforward and similar to the first reaction. The product has two short Mg–N_{Pyrn} bonds of 233 and 236 pm and one Mg–N_{Pyr} bond of 234 pm (the other Mg–N_{Pyr} interaction is 283 pm). The porphyrin strain energy has increased by 22 kJ mol^{-1}; however, it is 51 kJ mol^{-1} more stable than the reactant (4+0) complex. Therefore, the transition state is only 4 kJ mol^{-1} less stable than the reactant. The Mg–O bond length of the exchanging water molecule goes from 224 to 413 pm, through 254 pm in the transition state.

An alternative and better reaction path: The instability of the 4+0 complex and the stability of the 3+1 complex led us to study also an alternative reaction. It is conceivable that the second Mg–N_{Pyrn} bond does not form before the Mg–N_{Pyr} bond, owing to the favourable hydrogen bond to N_{Pyrn}. Therefore, we also tested the exchange of a fourth water molecule from a five coordinate complex, that is, the reaction 4+0,1N→3+1,1N (Figure 5). The product (3+1,1N) has only one Mg–N_{Pyrn} bond of 210 pm; the two Mg–N_{Pyr} interactions are 315 and 332 pm. On the other hand, it has three strong bonds to water, 194–203 pm. Thus, it is essentially four-coordinate. The porphyrin strain is quite high, 52 kJ mol^{-1}, but it is slightly (5 kJ mol^{-1}) more stable than the 4+0,1N complex.

The corresponding transition state represents a normal solvent-exchange reaction, in which one Fe–O distance increases from 215 to 377 pm, through 272 pm in the transition state. The transition state is 20 kJ mol^{-1} less stable than the

Figure 4. The fourth reaction of Mg: 4+0 to 3+1.

Figure 5. The alternative third reaction of Mg: 4+0,1N to 3+1,1N.

reactant complex. This energy is only slightly larger than that found for the 4+0→3+1 reaction.

Therefore, we continued to study the 3+0,1N→3+0,2N reaction (Figure 6). This reaction is similar to the corresponding 4+0 reaction in Figure 3. The length of the formed Mg–N_{Pyrn} bond goes from 361 to 233 pm through 287 pm in the transition state. The latter is 30 kJ mol^{-1} less stable than the reactant, whereas the product is 17 kJ mol^{-1} less stable. Thus, it is appreciably more favourable to go via the 3+1,1N complex than via the 4+0 complex; the maximum barrier is reduced from 82 to 30 kJ mol^{-1}.

It is possible that the strong destabilisation of the the 4+0 complex is an artefact of the small models used in this investigation (i.e., with many more water molecules, the coordinatively unsaturated 4+1,1N and 3+1,1N complexes may be destabilised). However, the important result of this part of the investigation is that there is a low-energy path for the formation of the second and third Mg–N bonds, indicating that the formation of the first Mg–N_{Pyrn} bond is the rate-limiting step. This is in accordance with experimental data.[10,11,13,14]

Formation of the fourth Mg–N bond: The fourth Mg–N bond is formed when the fourth water molecule is moved into the second coordination sphere, which we model as the 3+0→2+1 reaction in Figure 7. The product is almost symmetric with two short Mg–N_{Pyrn} bonds of 223 pm and two longer Mg–N_{Pyr} bonds of 242 and 244 pm. The two Mg–O bonds are 209 and 210 pm. It is 6 kJ mol^{-1} more stable than the reactant complex. The porphyrin strain energy is 150 kJ mol^{-1}.

The transition state is intermediate between the two structures: the Mg–N_{Pyr} bond has decreased from 281 to 255 pm and the Mg–O bond has increased from 219 to 272 pm. It is 19 kJ mol^{-1} less stable than the reactant complex. Thus, this reaction is far from rate-limiting.

Exchange of the fifth water molecule: In the porphyrin, the Mg ion can only keep one of the water molecules in the first coordination sphere (it is likely that it will eventually take up another water molecule on the other side of the porphyrin ring plane). Therefore, one more water molecule has to move into the second coordination sphere. We have also included this reaction, 2+0→1+1, in our investigation, depicted in Figure 8. This reaction is similar to the other reactions of the same type. Thus, the Mg–O distance increases from 213 to 413 pm through 272 pm in the transition state. This change is accompanied by a shortening of the Mg–N_{Pyrn} and Mg–N_{Pyr} bonds from 222 and 236–237 to 215 and 228 pm, respectively. The reaction is almost thermoneutral ($\Delta G = +2$ kJ mol^{-1}) and the transition state is only 19 kJ mol^{-1} above the reactant.

The first deprotonation of the porphyrin ring: We have seen how the four Mg–N bonds can be formed by successive movement of water molecules into the second coordination sphere of the Mg ion. The next step in the formation of Mg–porphyrin complex should be the displacement of the two pyrrole hydrogen atoms by some base. In principle, this can happen in any step of the previous reactions, that is, for intermediates with six to one water molecules. However, it seems most likely that the deprotonation takes place after the formation of the four Mg–N bonds. This is also in accordance with the deprotonation energies presented in Table 2. They show that the proton affinities (uncorrected energies in water) of the various complexes decreases with

Figure 6. The alternative fourth reaction of Mg: 3+0,1N to 3+0.

Figure 7. The fifth reaction of Mg: 3+0 to 2+1.

Figure 8. The sixth reaction of Mg: 2+0 to 1+1.

the number of water molecules, so that it is most likely that the proton is removed in the 2+0 or 1+0 complexes. Therefore, we have modelled this reaction for the 2+0 complex.

The proton acceptor in this reaction depends on the system of interest. In pure water, it must be a water molecule. In ferrochelatase, several different residues have been suggested, for example, His-183 and Tyr-13 (numbering according to the enzyme from *Bacillus subtilis*).[9,44] In this investigation, we have tested two different molecules. imidazole (Im) and water (Wat). This choice is quite arbitrary, but imidazole has an intermediate pK_a(~7.0),[45] whereas water is the ultimate acceptor of the proton in solution. Thus, our choice should not be interpreted as that we suggest that His is the proton acceptor in ferrochelatase. Instead, we want to test different alternatives and get a feeling of the barriers involved.

The first proton transfer from pyrrole to imidazole is a simple and pure reaction, as can be seen in Figure 9. Before the reaction, imidazole is hydrogen-bonded symmetrically to the two pyrrole hydrogen atoms with a N_{Im}–H distance of 196–197 pm and with N_{Pyr}–H bonds of 106 pm. After the reaction, there is a N_{Im}–H bond of 106 pm and a N_{Pyr}–H hydrogen bond of 187 pm. At the same time, the corresponding Mg–N bond length decreases from 237 to 214 pm, accompanied by an increase in the other Mg–N bond lengths. The transition state is reactant-like with N_{Im}–H and N_{Pyr}–H distances of 151 and 117 pm. It has a single imaginary frequency of 74 cm^{-1}, showing a neat N–H–N reaction coordinate. The activation energy is only 0.1 kJ mol^{-1}, indicating that the reaction should be very rapid. The product state is 41 kJ mol^{-1} more stable than the reactant state.

Second deprotonation of the porphyrin ring: Next, we removed the protonated imidazole and added a new neutral imidazole (modelling the interchange of the proton with bulk solvent). This complex (Figure 10) formed a stronger hydrogen bond than that of the reactant in the previous reaction, with a N_{Im}–H distance of 165 pm and a N_{Pyr}–H bond of 110 pm. In the product the distances are almost inverted, and in the transition state the two distances are almost equal, 133 and 128 pm. Without any corrections, the barrier for the reaction is 4 kJ mol^{-1}. However, with the corrections, the transition state actually becomes 1 kJ mol^{-1} more stable than the reactant. The product is 17 kJ mol^{-1} more stable than the reactant complex.

Interestingly, the product is not the magnesium–porphyrin complex, but instead a SAT complex with three short Mg–N_{Pyrn} distances of 216–218 pm and one longer distance of 224 pm. This last bond is to the N_{Pyrn} atom that forms a hydrogen bond to the protonated imidazolium cation. The two Mg–O distances are 219 and 229 pm. However, when the imidazolium ion is removed, the complex spontaneously (without any barrier) reorganises to a 1+1 complex with four Mg–N_{Pyrn} bonds of 210–212 pm and a Mg–O bond of 210 pm (Figure 13). Owing to the fact that the Mg ion is only five-coordinate, without any ligand below the porphyrin ring, it is displaced 34 pm out of the porphyrin plane towards the water ligand. The porphyrin strain is 6 kJ mol^{-1} (relative to free

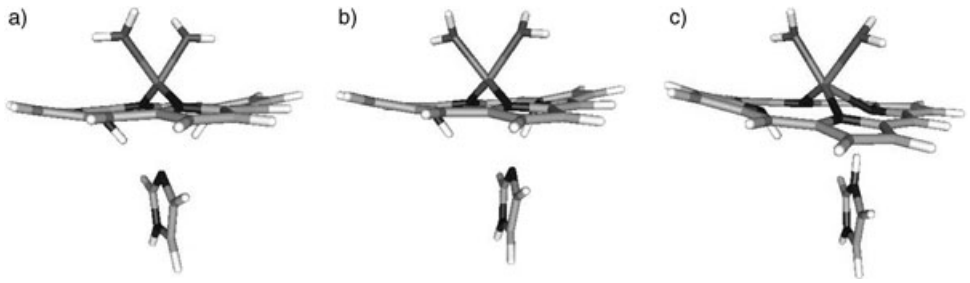

Figure 9. The first deprotonation of Mg 2+0 by imidazole.

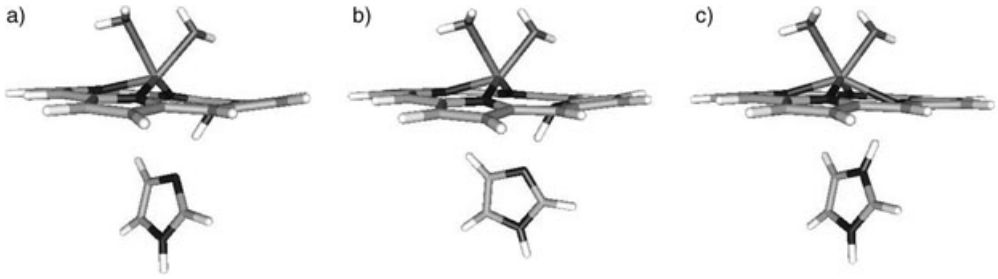

Figure 10. The second deprotonation of Mg 2+0 by imidazole.

Por^{2-}). If the second-sphere water molecule is removed, the Mg ion moves closer to the ring plane (25 pm above the mean plane). However, when this water ligand is also removed, the Mg ion moves into the ring plane.

Deprotonation by water: If we use water as the proton acceptor instead, the energetics change appreciably. In particular, both deprotonations become strongly uphill (by 70–74 kJ mol^{-1}). The energy goes steadily up when the protons are moved from the porphyrin to water, so no transition structure could be found for any of the reactions. The reactants and the products are shown in Figure 11 and 12. The

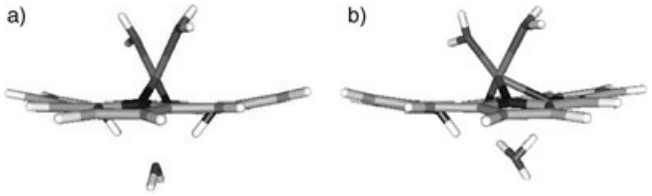

Figure 11. The first deprotonation of Mg 2+0 by water.

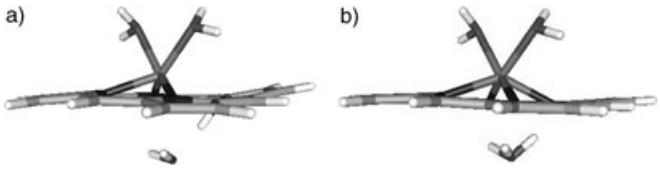

Figure 12. The second deprotonation of Mg 2+0 by water.

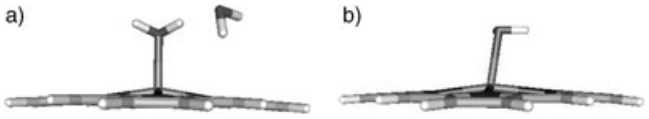

Figure 13. The fully deprotonated Mg 1+1 and 1+0.

same applies if the deprotonation takes place in the complex with only one water molecule (75–80 kJ mol^{-1}, see Table 2). However, some of the effects seem to come from an unfavourable interaction between H_3O^+ and the porphyrin complex. If we calculate the energies only for the separated reactants and products ($H_2OFePorH_2^{2+} + H_2O \rightarrow H_2OFePorH^+ + H_3O^+$), at least the first deprotonation is only slightly uphill (24 kJ mol^{-1}), whereas the second deprotonation is still strongly uphill (85 kJ mol^{-1}). Unfortunately, these energies are quite uncertain with large solvation effects.

These results clearly show the importance of having a proton acceptor with a proper acidity. For our simplified model systems, imidazole is more basic than the sitting-atop complexes, whereas water is not. It is likely that the deprotonation may be facilitated by hydrogen-bonded networks, which may rapidly transport the proton away from the sitting-atop complexes.

The metallation reactions with Fe^{2+}: Next, we repeated all the calculations also with Fe^{2+}, that is, we studied the metallation of $PorH_2$ by $Fe(H_2O)_6^{2+}$. The results of this investigation are presented in Figure 14 and in Tables 3 (geometries) and 4 (energies). Most of the reactions are completely analogous to the corresponding reactions for Mg^{2+}. In this section, we will therefore concentrate on the notable differences.

The most conspicuous difference is that Fe decreases the proton affinity of its water ligands. Therefore, it is observed in many complexes that one of the water ligands donates one of its protons to $PorH_2$, forming a $FeOHPorH_3^+$ complex. In some cases, both the $FeOH_2PorH_2$ and $FeOHPorH_3^+$ forms exists, whereas in others, only the latter form can be obtained (unless constraints are introduced). In particular, all 1N complexes, are of the latter type. This adds a complication to some of the reactions (e.g. the n+0,1N → n+0,2N reactions), because they will involve both a change in the iron ligand sphere and a transfer of a proton. Therefore, the reactants and transition states of these reactions (from 4+0,1N and 3+0,1N) have been obtained by constraining the transferred proton to reside on the water molecule.

The first notable difference between Mg and Fe is the structure of the outer-sphere 6+0 complex. As can be seen by comparing Figures 1 and 14a, these two complexes have slightly different structures. In the Mg complex, a water molecule forms hydrogen bonds to both the N_{Pyrn} atoms, whereas in the Fe complex, two different water molecules form a hydrogen bond to each of the N_{Pyrn} atoms. We have confirmed that the complexes actually are different and true minima by performing a frequency analysis (no imaginary

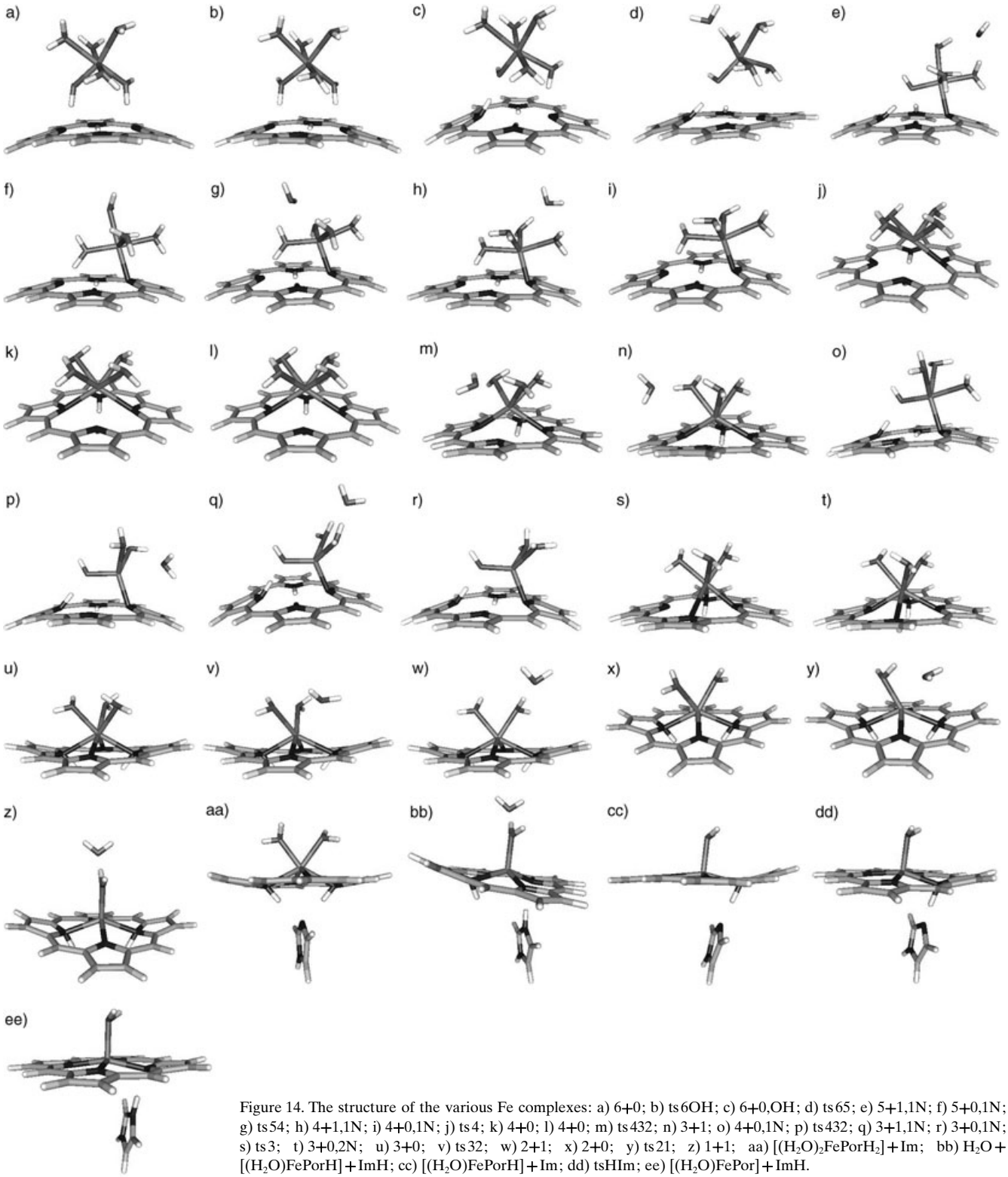

Figure 14. The structure of the various Fe complexes: a) 6+0; b) ts6OH; c) 6+0,OH; d) ts65; e) 5+1,1N; f) 5+0,1N; g) ts54; h) 4+1,1N; i) 4+0,1N; j) ts4; k) 4+0; l) 4+0; m) ts432; n) 3+1; o) 4+0,1N; p) ts432; q) 3+1,1N; r) 3+0,1N; s) ts3; t) 3+0,2N; u) 3+0; v) ts32; w) 2+1; x) 2+0; y) ts21; z) 1+1; aa) $[(H_2O)_2FePorH_2]+Im$; bb) $H_2O+[(H_2O)FePorH]+ImH$; cc) $[(H_2O)FePorH]+Im$; dd) tsHIm; ee) $[(H_2O)FePor]+ImH$.

frequencies) and by interchanging the metals and reoptimising.

Moreover, for Fe another form of the 6+0 complex exists in which the proton on one of the hydrogen-bonded water molecules has been transferred to the N_{Pyrn} atom. We call this complex 6+0,OH (Figure 14c). It is actually 6 kJ mol^{-1} more stable than the normal 6+0 complex. The transition state between these two structures is only 1 kJ mol^{-1} less stable than the 6+0 complex. Moreover, the 6+0,OH complex is actually the starting point of the first ligand exchange

Table 3. Fe–ligand distances [pm] in the studied Fe complexes.

	$Fe–N_{Pyrn}$	$Fe–N_{Pyr}$	Fe–O
6+0	427.7, 429.3	409.0, 457.9	204.3, 204.6, 218.6, 218.9, 219.9, 229.9
ts6OH	426.7, 429.9	406.4, 461.6	202.5, 206.1, 219.3, 219.9, 220.7, 228.4
6+0,OH	429.9, 450.1	419.1, 467.2	190.1, 217.6, 219.2, 222.7, 227.7, 231.2
ts65	377.4, 467.9	428.2, 433.7	190.3, 215.5, 217.7, 221.1, 222.6, 277.9
5+1,1N,OH	224.1, 451.0	362.7, 367.5	193.8, 218.9, 219.2, 223.2, 228.1, 381.9
5+0,1N,OH	225.4, 451.3	364.4, 367.0	192.9, 217.3, 220.5, 226.6, 227.8
ts54	211.4, 409.0	340.7, 350.6	196.3, 218.2, 220.2, 224.5, 291.2
4+1,1N,OH	215.6, 428.8	347.3, 355.7	188.5, 212.7, 222.2, 226.8
4+0,1N constr.	201.7, 409.3	334.2, 338.8	212.4, 212.6, 214.5, 224.6
ts4	215.7, 294.3	245.9, 302.7	222.7, 223.8, 224.7, 227.3
4+0	237.0, 238.0	258.7, 259.9	228.7, 229.1, 229.4, 229.7
4+0	237.0, 238.0	258.7, 259.9	228.7, 229.1, 229.4, 229.7
ts432	231.8, 235.3	251.1, 258.9	224.7, 227.4, 233.7, 252.8
3+1	223.1, 226.2	241.8, 252.6	224.6, 225.3, 226.2, 437.9
4+0,1N,OH	215.4, 429.4	351.5, 352.2	187.7, 220.3, 220.5, 225.3
ts431	209.3, 417.0	340.5, 341.3	187.8, 213.2, 216.5, 273.2
3+1,1N,OH	208.4, 403.9	331.9, 332.4	186.2, 208.9, 210.3, 389.1
3+0,1N,OH	206.0, 405.9	331.0, 334.1	185.2, 212.5, 213.7
3+0,1N constr.	200.2, 378.4	298.8, 326.4	197.5, 209.2, 211.5
ts3	208.0, 275.8	228.5, 292.2	212.8, 216.6, 222.7
3+0	221.2, 223.6	238.5, 256.3	223.1, 225.3, 231.7
3+0,1N,OH	206.0, 405.9	331.0, 334.1	185.2, 212.5, 213.7
ts3*cis*	201.9, 242.9	336.7, 353.1	204.9, 211.5, 215.4
3+0*cis*	205.5, 205.6	342.3, 344.7	213.9, 220.3, 222.2
3+0	221.2, 223.6	238.5, 256.3	223.1, 225.3, 231.7
ts32	219.1, 223.2	240.2, 241.2	222.7, 223.7, 260.6
2+1	214.8, 215.6	241.9, 243.5	213.3, 217.3, 413.8
2+0	214.2, 214.3	239.6, 239.7	217.4, 217.5
ts21	211.6, 212.3	233.7, 236.5	210.8, 252.2
1+1	208.9, 209.6	228.6, 229.7	200.9, 409.9

	$Fe–N_{Pyrn}$	$Fe–N_{Pyr}$	Fe–O	$N_{Pyr}–H$	$N_{Im}–H$
$[(H_2O)_2FePorH_2]+Im$	213.6, 213.7	236.1, 238.9	216.3, 220.8	105.5, 105.7	197.1, 200.5
$(H_2O)+[(H_2O)FePorH]+ImH$	208.1, 208.7	206.9, 238.4	204.1, 411.4	102.9, 193.7	105.1, 414.5
$(H_2O)+[(H_2O)FePorH]+Im$	205.6, 206.0	202.8, 231.5	208.1, 375.6	109.8	166.8
tsHIm	206.8, 207.2	204.7, 225.8	207.8, 374.7	127.2	133.5
$(H_2O)+[(H_2O)FePor]+ImH$	207.8, 209.1	206.1, 216.4	208.6, 378.4	172.5	108.0
$[(H_2O)FePorH]+Im$	200.0, 204.7	205.0, 232.7	215.8	109.8	166.5
tsHIm	201.6, 205.6	206.8, 226.1	215.3	125.2	135.3
$[(H_2O)FePor]+ImH$	203.9, 207.4	208.7, 213.8	216.1	176.4	107.3

	$Fe–N_{Pyrn}$	$Fe–N_{Pyr}$	Fe–O	$N_{Pyr}–H$	$O_{Wat}–H$
$[(H_2O)_2FePorH_2]+H_2O$	208.0, 208.2	226.5, 227.0	207.7	104.6, 104.8	197.9, 203.8
$[(H_2O)_2FePorH]+H_3O$	206.2, 213.7	214.9, 234.1	208.2	103.0, 151.9	104.7, 302.9
$[(H_2O)_2FePorH]+H_2O$	200.3, 205.6	205.7, 237.2	214.4	105.1	177.4
$[(H_2O)_2FePor]+H_3O$	206.6, 207.3	215.4, 224.3	212.7	143.7	108.8
$[(H_2O)FePor]$	205.6, 206.6	207.9, 208.6	223.6		
[FePor]	206.2, 206.2	206.2, 206.2			

reaction, which has an appreciably lower barrier for Fe than for Mg (33 versus 72 kJ mol^{-1}).

The rest of the reactions for Fe are similar to those with Mg (cf. Figure 14). The energies of the various reaction steps for Mg and Fe are compared in Figure 15. Thus, the path through the 3+1,1N complex is much more favourable than the path through the 4+0,2N complex. The other reactions have barriers of 4–51 kJ mol^{-1}. The highest barrier is observed for the the 3+0,1N→3+0,2N isomerisation and is caused mainly by the stability of the 3+0,1N complex (reaction energy 43 kJ mol^{-1}). Thus, this step has a higher barrier than the first step, in contrast to Mg. However, it is likely that the relative stabilities of the 3+0,1N and 2N complexes will change if more water molecules are included in the calculations. Moreover, the 3+0,1N→3+0,2N isomerisation may be facilitated in aqueous solution, because then the $N_{Pyrn}\cdots H–O$ hydrogen bond (in the 3+0,1N complex) will be less important, because it can be replaced by hydrogen bonds to water instead.

In the first deprotonation of the porphyrin by imidazole, starting from the complex with two water molecules (2+0), no barrier was found. Moreover, one of the water ligands moved into the second coordination sphere of Fe during the reaction (Figure 14bb). A final difference between Mg and Fe is that for the latter metal ion, there is a much stronger stabilisation (exothermic reaction energy) of the last complexes in the reaction (the 1+1 complex and the two deprotonation products). Thus, the total reaction is ~100 kJ mol^{-1} more exothermic for Fe than for Mg. This indicates that it is easier to deprotonate the porphyrin ring with Fe than with Mg. This may also explain, together with the lower activation barrier for Fe, why there is a need for ATP in magnesium chelatase, but not in ferrochelatase.[4–9] However, deprotonation by water is still strongly unfavourable (Table 4).

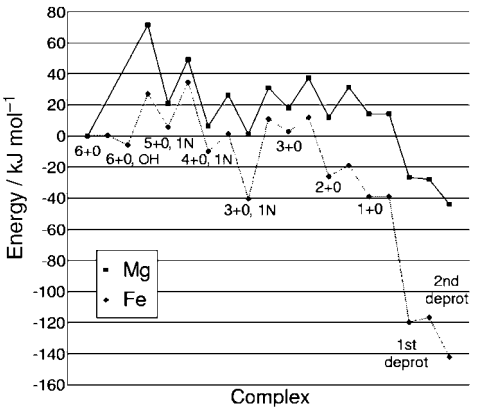

Figure 15. The reaction and activation free energies of the various reaction steps for the Mg^{2+} (full line) and Fe^{2+} (dashed line) complexes.

The effect of water on the opposite side: We have previously found that the porphyrin ring becomes quite distorted if it is allowed to form hydrogen bonds to water molecules through the central nitrogen atoms (strain energy 70–75 kJ mol^{-1}).[43] It is conceivable that such a distortion may significantly facilitate the metallation of the porphyrin ring (also in the chelatases, in which there is a strategically located Tyr-13 residue). We therefore repeated the calculations of first reaction step with Mg (which is rate-limiting in this system) with a water molecule on the side of the porphyrin opposite to the metal ion, forming two symmetric hydrogen bonds to the pyrrole hydrogen atoms (Figure 16).

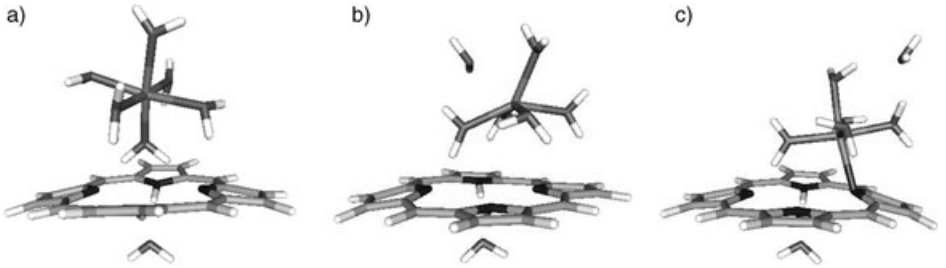

Figure 16. The first reaction of $Mg(H_2O)_6$ with $PorH_2$, 6+0 to 5+1,1N with an extra water molecule on the side of the porphyrin opposite to the Mg ion.

However, as can be seen in Table 2, this did not change the reaction energies significantly: The activation barrier is still 71 kJ mol^{-1} and the reaction energy is 16 kJ mol^{-1} (72 and 21 kJ mol^{-1} without the extra water molecule). Therefore, water molecules on the opposite side of the porphyrin ring do not seem to affect the reaction energies significantly. Yet, there is a clear distortion of the complex by the extra water molecules: the porphyrin strain energy increases by ~36 kJ mol^{-1} in both the reactant and the product complexes.

Metallation of a methylated porphyrin ring: Likewise, it is known that already distorted porphyrin rings (e.g., by bulky side-chains or substituents on the pyrrole nitrogen atoms) have a 10^3–10^5 higher rate of metallation than undistorted ring systems.[15] In order to look for the source of this effect, we have also studied the first reaction step for Mg with a porphyrin ring methylated on one of the two pyrrole rings ($PorHCH_3$, Figure 17). However again, we do not see any significant increase in the reaction rate of this step: On the contrary, both the activation and reaction energies increase by ~10 kJ mol^{-1} (to 83 and 31 kJ mol^{-1}, as can be seen in Table 2). However, as expected, the strain energy of the porphyrin ring (this time compared to the free $PorHCH_3$ ring) decreases by ~4 kJ mol^{-1}.

The reason why we do not see any significant effect of the distortion of the porphyrin ring is probably that the 6+0 and 5+0,1N complexes have a similar and quite low strain energies, 27–34 kJ mol^{-1}. Effects of a distortion of the porphyrin ring would be expected primarily when the strain energy changes during the reaction. Therefore, we also studied the 3+0,1N→3+0,2N reaction step, in which the porphyrin strain energy increases from 75 to 120 kJ mol^{-1} (Figure 18). In this case, we obtained a somewhat larger effect of the methylation of the porphyrin ring: The reaction energy decreased from 17 to 9 kJ mol^{-1} and the activation energy decreased from 30 to 27 kJ mol^{-1} (the effect is larger without the corrections: from 5 to 16 kJ mol^{-1} for the reaction energy and from 14 to 7 kJ mol^{-1} for the activation energy). This is accompanied by a decrease in the porphyrin strain energy from 75 to 73 kJ mol^{-1} for the reactant and from 120 to 91 kJ mol^{-1} for the product. Thus, we see some effect of the methylation in this step, even if it is not very large.

Conclusion

In this paper, we have studied the metallation of a porphyrin by a fully solvated metal ion,

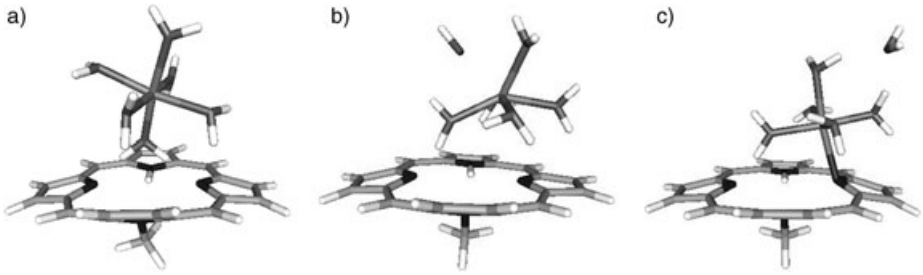

Figure 17. The first reaction of $Mg(H_2O)_6$ with the methylated $PorHCH_3$ ring: 6+0 to 5+1,1N.

Table 4. Energies of the optimised Fe^{2+} complexes. The entries are explained in the legend of Table 2.

	ΔE	$\Delta\Delta$Solv	$\Delta\Delta$Method	$\Delta\Delta$Thermal	ΔG	ΔE_{Porph}	Imag f
$Fe(H_2O)_6+PorH_2$	0.0	−233.6	−52.7	−65.7	−99.4	0.0	–
6+0	0.0	0.0	0.0	0.0	0.0	31.1	–
ts6OH	0.1	−0.4	2.5	−1.6	0.5	–	79.1
6+0,OH	−20.3	19.1	−4.4	−0.2	−5.8	18.1	–
ts65	1.2	14.3	3.6	8.1	27.3	–	60.0
5+1,1N,OH	−59.1	19.3	21.7	24.0	5.8	–	–
5+0,1N,OH	0.0	0.0	0.0	0.0	0.0	68.7	–
ts54	36.7	−2.9	−1.2	−3.8	28.8	–	−64.7
4+1,1N,OH	−5.6	13.6	−9.2	−14.5	−15.7	–	–
4+0,1N constr.	0.0	0.0	0.0	0.0	0.0	45.4	–
ts4	47.6	2.8	13.7	13.3	77.5	–	102.4
4+0	41.5	5.8	14.5	12.6	74.4	91.5	–
4+0	0.0	0.0	0.0	0.0	0.0	91.5	–
ts432	1.5	0.5	0.2	0.7	3.0		41.4
3+1	−29.0	7.0	−16.8	−9.2	−48.0	–	–
4+0,1N	0.0	0.0	0.0	0.0	0.0	45.4	–
ts431	7.4	2.9	0.7	0.5	11.5	–	100.8
3+1,1N	−33.4	10.9	−5.8	−2.2	−30.4	–	–
3+0,1N	0.0	0.0	0.0	0.0	0.0	59.0	–
3+0,1N constr.	27.0	−13.5	2.9	−8.1	8.2	–	–
ts3	55.6	−11.4	−0.2	7.3	51.3	–	80.5
3+0	42.6	−8.1	−1.1	9.7	43.1	134.5	–
3+0,1N	0.0	0.0	0.0	0.0	0.0	59.0	–
ts3 *cis*	95.1	−11.0	13.7	−8.6	89.1	–	1442.6
3+0 *cis*	25.5	−5.0	0.5	−0.6	20.4	–	–
3+0	0.0	0.0	0.0	0.0	0.0	134.5	–
ts32	4.3	2.1	0.5	2.4	9.2	–	88.8
2+1	−24.0	8.0	−7.3	−5.6	−28.9	–	–
2+0	0.0	0.0	0.0	0.0	0.0	167.2	–
ts21	0.2	1.1	6.2	0.4	7.2	–	90.9
1+1	−35.4	18.5	4.4	−0.4	−12.9	–	–
1+0	–	–	–	–	–	191.4	–
$[(H_2O)_2FePorH_2]+Im$	0.0	0.0	0.0	0.0	0.0	–	–
$(H_2O)+[(H_2O)FePorH]+ImH$	−72.9	3.3	−3.2	−8.0	−80.7	–	–
$(H_2O)+[(H_2O)FePorH]+Im$	0.0	0.0	0.0	0.0	0.0	–	–
tsHIm	4.4 (−0.1)[a]	−4.8	6.5	−3.1	3.0	–	802.9
$(H_2O)+[(H_2O)FePor]+ImH$	−7.0 (−25.3)[a]	−19.6	0.0	4.2	−22.5		
$[(H_2O)FePorH]+Im$	0.0	0.0	0.0	0.0	0.0	–	–
tsHIm	3.9	−4.6	6.1	−7.1	−1.7	–	750.4
$[(H_2O)FePor]+ImH$	−9.4	−21.1	−1.8	3.6	−28	–	–
$[(H_2O)FePorH_2]+H_2O$	0.0	0.0	0.0	0.0	0.0	–	–
$[(H_2O)FePorH]+H_3O$	0.0	−20.3	12.6	−1.4	68.9	–	–
$[(H_2O)FePorH]+H_2O$	0.0	0.0	0.0	0.0	0.0	–	–
$[(H_2O)FePor]+H_3O$	0.0	−5.7	8.7	7.5	70.7	–	–
$[(H_2O)FePor]$	–	–	–	–	–	15.3	–
[FePor]	–	–	–	–	–	14.2	–

[a] For the intermediate-spin triplet state.

Mg^{2+} or Fe^{2+}. The results provide some interesting insights into this important reaction. First, we note that rate-limiting step for the Mg reaction is the exchange of the first ligand. This is in accordance with available experimental

Figure 18. The fourth reaction of Mg with the methylated PorHCH$_3$ porphyrin: 3+0,1N to 3+0.

data.[10,11,13,14] The calculated activation energy is 72 kJ mol^{-1}. This is similar to the activation energy estimated for porphyrin metallation by Mg catalysed by pyridine, 66 kJ mol^{-1}.[3] Pyridine probably catalyses the deprotonation of the porphyrin ring, which otherwise may become rate limiting, as we saw for deprotonation with water.

For Fe, the formation of the first bond between Fe and the porphyrin has an appreciably lower activation energy of 33 kJ mol^{-1}. However, the next step (5+0,1N→4+1,1N) has a slightly higher barrier (40 kJ mol^{-1}, calculated from the 6+0,OH complex) and the 3+0,1N→3+0,2N isomerisation has an even higher barrier, 51 kJ mol^{-1}. In the isomerisation step, we essentially go from one to four Fe–porphyrin bonds in one step (the three Fe−N distances change from 331–409 pm to 224–256 pm). It is probable that this barrier is an artefact of the small model systems that gives a too high stability of complexes with a low coordination number. However, the results are fully consistent with the fact that the metallation of a porphyrin is appreciably faster with Fe than with Mg.[3]

The other steps of the metallation reaction have lower activation barriers. Thus, these reactions are faster than the first exchange reaction, and should therefore be of little mechanistic significance. Likewise, the barriers for the deprotonation are less than 1 kJ mol^{-1} if the proton acceptor is imidazole. Therefore, these reactions should also be rapid provided that there are proton acceptors in the solvent and that the pH is not too low.

Interestingly, we see no evidence for a preceding equilibrium between a planar and deformed porphyrin ring; no local minimum with a distorted porphyrin ring was found. In fact, the barrier for the first step of the metallation reaction, the formation of the first bond between the metal and the porphyrin, is not even reduced if the porphyrin is distorted by methylation of one of the pyrrole nitrogen atoms or by hydrogen bonds on the side opposite to the metal ion. However, the porphyrin is strongly distorted in the intermediates, by 27–195 kJ mol^{-1}. This indicates, that the deformation energy is included in the activation and reaction energies of all the reaction step, rather than being a multiplicative equilibrium factor.[43] It is notable that these well-defined strain energies are appreciably higher than what has been experimentally estimated, 10–30 kJ mol^{-1}.[14,46]

It has been discussed whether the ligand-exchange reactions during the metallation are dissociative or associative.[12] Although we have not systematically investigated these competing mechanisms for all steps, we have found low barriers for most ligand-exchange reactions with a concerted mechanism, whereby the new bond is formed in the same step as the old bond is broken (cf. Figure 1). However, for the formation of the second bond to the porphyrin ring (the chelate formation), a dissociative mechanism seems to be necessary, owing to the strong hydrogen bond between a metal-bound water molecule and the other N_{Pyrn} atom in the 1N complexes (the 4+1,1N complex has a five-coordinate metal ion). Moreover, our results indicate that a doubly dissociative mechanism is most favourable, that is, the lowest barriers are found if we go via the 3+0,1N complex (which has a four-coordinate metal ion). However, as discussed above, this may be an artefact of the small model systems used.

Our results indicate that the reaction mechanism is more complicated than what is normally assumed, namely, involving individual steps for the exchange of each of the five water molecules that has to leave the metal ion before the four bonds to the porphyrin complex can be formed. In addition, there must be two deprotonation steps (as has been recognised before) and one step going from the stable 1N complexes (with only one Fe−N_{Pyrn} bond, whereas the second N_{Pyrn} atom forms a hydrogen bond to one of the metal-bond solvent molecules) to a complex with two Fe−N_{Pyrn} bonds. Thus, the full mechanism should involve nine steps (if we include also the formation of the outer-sphere complex), rather than the six steps normally discussed.[10–14] This reaction mechanism is summarised in Table 5.

Table 5. Suggested reaction mechanism for the metallation of porphyrins, starting from a six-coordinate metal ion. Note that the order of the steps (especially the position of steps 5, 8 and 9 relative to steps 3, 4, 6 and 7) is not fixed. Step 10 is optional.

Step	Reaction
1	Formation of an outer-sphere complex of the hydrated metal and the porphyrin.
2	Formation of the first metal–porphyrin bond by the exchange of one water ligand.
3	Exchange of the second water ligand.
4	Exchange of the third water ligand.
5	Formation of the second metal–porphyrin bond (going from a 1N to a 2N complex).
6	Exchange of the fourth water ligand.
7	Exchange of the fifth water ligand.
8	Deprotonation of the third pyrrole ring of the porphyrin.
9	Deprotonation of the fourth pyrrole ring of the porphyrin.
10	Formation of a second axial bond of the metal on the opposite side of the porphyrin ring.

Finally, it should be noted that other types of complexes may also be involved in the reaction mechanism, for example, complexes in which the metal ion is coordinated to two different porphyrin rings or complexes in which the two protons in the centre of the porphyrin ring reside on nitrogen atoms that are in *cis*, rather than *trans*, positions. In our previous quantum mechanical study, no complex with two porphyrin rings were found for Mg, whereas they were found but were energetically unfavourable for Fe.[43] However, the *cis* complexes with three and four water molecules are more stable than the corresponding *trans* complexes for both Mg and Fe (by 14–45 kJ mol^{-1}), but still slightly less stable than the corresponding 1N complexes, except for the Mg 3+0 complexes. Thus, it is possible that the barrier of our rate-limiting step for Fe (3+0,1N→3+0,2N) is reduced by ~18 kJ mol^{-1}[43] by involving the 3+0 *cis* complex. We have tried to model such a *trans–cis* isomerisation for the 3+0 1N complex (Figure 19 and Table 4). However, the barrier for this step turned out to be prohibitively high (89 kJ mol^{-1}). It is also possible that the isomerisation from the *trans* to the *cis* porphyrin is facilitated or avoided by deprotonation of the porphyrin ring. The matter may be even more complicated by coupling to the proton transfer between the porphyrin ring and the metal-bound water molecules, observed for the Fe complexes. For these reasons, we have not proceeded with these studies further.

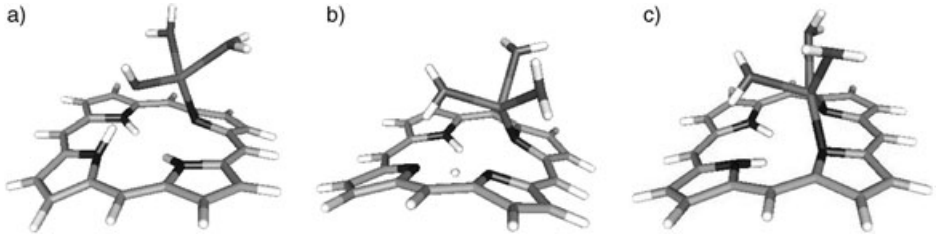

Figure 19. The fourth reaction of Fe with $PorH_2$, involving an isomerisation between *trans* and *cis* form of the 3+0 complex (*trans* 3+0,1N to *cis* 3+0).

The present calculations also give some clues to the metallation reactions taking place in the magnesium chelatase and ferrochelatase enzymes. First, we have seen that the main problem in the metallation is to get rid of the original water solvation shell. In ferrochelatase, it seems that parts of this desolvation takes place during the binding of the metal to the enzyme. Recent crystallographic studies with zinc and cadmium have identified a metal-binding site close to the porphyrin site, but with only four (Zn) or five (Cd) ligands, His-183, Glu-264, Tyr-13 (only Cd) and two or three water molecules.[47] These studies were performed without any porphyrin (otherwise, the metal would be directly incorporated into the porphyrin ring), which may change the results somewhat (Tyr-13, which is involved in the binding of Cd only, resides on the opposite side of the porphyrin when it is bound).[44] Thus, it is likely that Fe^{2+} binds to His-183 and Glu-264 together with 1–3 solvent molecules in the ferrochelatase–porphyrin complex, implicating a reduction of the coordination number to 3–5. Clearly, this will facilitate the metallation of the porphyrin ring. In crystal structures of ferrochelatase, a fully solvated Mg ion is found ~700 pm from the Zn site. It is possible that this also represents a intermittent binding site for a fully solvated Fe^{2+} ion, during its binding to the metal site close to the porphyrin ring, and that 3–5 water molecules are stripped of the metal ion during its movement to His-183 and Glu-264. However, it should also be mentioned that other groups have suggested that the metal rather binds on the opposite side of the porphyrin ring, with Tyr-13 and His-88 as a possible ligands.[48]

Second, our calculations also indicate that there needs to be a proper group for the deprotonation of the porphyrin ring in the protein. This group should be on the side of the porphyrin ring opposite to the metal ion. If the metal binds to His-183 and Glu-283, then Tyr-13 is the most likely candidate. It is located only 312 pm from one of the N atoms in the porphyrin ring.[47] Another candidate on this side of the porphyrin ring is His-88 (590 pm). On the opposite side of the ring there are only the two putative Zn ligands His-183 (377 pm) and Glu-264 (561 pm). In addition, there are a number of water molecules around the porphyrin ring (especially opposite to the Zn site), with a distance of down to 330 pm to the porphyrin N atoms. From mutation studies, it is known that His-183 and Glu-264 are essential for the reactivity, whereas a Tyr13Phe mutant has only 20–30% lower activity than the wild-type enzyme (M. Hansson, unpublished data). This gives some strength to the suggestion of His-183 and Glu-264 as metal-binding residues, but indicates that the porphyrin ring is probably deprotonated directly by the water molecules available in the binding cleft. This indicates that the deprotonation of the porphyrin in the protein is easier than in pure water. We are currently studying the ferrochelatase reaction in the protein with combined quantum and molecular mechanics (QM/MM) methods.

Computational Methods

We have studied the metallation of a porphyrin ($PorH_2$, that is, a porphyrin ring without any side chains) with Mg^{2+} (the central ion in chlorophyll) and Fe^{2+} (the central ion in haem). The metal has been allowed to coordinate to 1–6 water molecules. In addition, we have studied the deprotonation of $PorH_2$ by an imidazole (Im) group or a water molecule. Complexes between a metal ion, $PorH_2$ and a number of water molecules are denoted by $n+m$, in which n and m are the number of first- and second-sphere water molecules of the metal ion.

Geometry optimisations were performed with the density functional BP86 method, which consists of Becke's 1988 gradient corrected exchange functional, combined with Perdew's 1986 correlation functional.[49,50] These calculations employed the 6-31G* basis set for all atoms, except for the metals, for which the TZVP (Mg) or the DZP (Fe) basis

sets of Schäfer et al. were used.[51,52] This last basis set was enhanced with one d, one f and two p-type functions with exponents of 0.1244, 1.339, 0.134915 and 0.041843. These calculations were sped up by expansion of the Coulomb interactions in auxiliary basis sets, the resolution-of-identity approximation.[53,54]

After the geometry optimisation, accurate energies were calculated by using the three-parameter hybrid functional B3LYP, as implemented in the Turbomole package.[55] In these calculations, the 6-311+G(2d,2p) basis set was used for the light atoms (including Mg) and the basis set for Fe was enhanced an s function with the exponent 0.01377232 and the single f function was replaced by two functions with exponents 2.5 and 0.8. Inclusion of diffuse functions during the geometry optimisation affected the relative energies by less than 1 kJ mol^{-1}.[43]

Density functional methods have been shown to give excellent geometries for transition-metal complexes (including haem models with various axial ligands), with errors in the bond distances of 0–7 pm.[56–58] In particular, the B3LYP method is known to give the most accurate energies of the widely used density functionals.[20,21,59] Calibrations on transition-metal complexes have shown that the geometries and energies do not change significantly if the method or the basis sets are improved from the present level.[60]

Solvation effects were estimated by single-point calculations by using the continuum conductor-like screening model (COSMO).[61,62] These calculations were performed at the same level of theory as the geometry optimisation and with default values for all parameters (implying a water-like probe molecule) and a dielectric constant (ε) of 80. For the generation of the cavity, a set of atomic radii had to be defined. We used the optimised COSMO radii in Turbomole (130, 200, 183 and 172 pm for H, C, N and O, respectively, and 200 pm for the metals).[63]

The zero-point energy and thermal corrections to the Gibbs free energy (at 298 K and 1 atm pressure, by using an ideal-gas approximation[64]) were calculated from a frequency calculation, obtained with the Gaussian 98 software,[65] with the same method and basis set as in the geometry optimisation. The same software was used for the optimisation of the transition-state structures, whereas all the other calculations were carried out with the Turbomole 5.6 software.[66] We made use of default convergence criteria in the respective program. Several starting structures were tried for most complexes, but only the structure with the lowest energy of each type is reported.

Calculations on iron were complicated by the presence of several possible spin states. For Fe^{2+} these are the low-spin singlet state, the intermediate-spin (IS) triplet state and the high-spin (HS) quintet state. With weak-field ligands, like water, Fe^{2+} attains a HS ground state, and Fe^{2+} is consequently HS in aqueous solution.[16,19] This also applies to most five-coordinate haem complexes, but FePor is known to have a IS ground state (with a low-lying excited HS state, which is stabilised by distortion of the haem ring) and six-coordinate haem complexes are in general low-spin, although water complexes may show a mixture of several spin states.[22,31,33] Therefore, we assumed that all iron complexes were HS and unrestricted open-shell theory was employed for these calculations.

However, the assumption was checked for several complexes. For example, the HS state is 122, 54 and 15 kJ mol^{-1} more stable than the IS state for the $[Fe(H_2O)_6]^{2+}$, $[FePorH_2(H_2O)]^{2+}$ and the $[FePorH(H_2O)]^{+}$ complexes, respectively (and the singlet state is even less stable). It is only for the $[FePor(H_2O)]$ complex that the triplet state is more stable than the HS state (by 12 kJ mol^{-1}), and it is not clear if this calculation may be trusted, because B3LYP indicates that a five-coordinate deoxyhaem model has a IS ground state, although experiments show that it should be HS.[22,24,33] However, these results clearly show that the HS state is appropriate for all reactions, except perhaps the final one. Therefore, we have also studied the last reaction $[(H_2O)FePorH)]+Im \rightarrow [(H_2O)FePor+ImH)]$ in the IS state, which changed the activation energy by less than 5 kJ mol^{-1} (Table 4).

Acknowledgement

This investigation has been supported by grants from the Swedish research council, by computer resources of Lunarc at Lund University, and by a scholarship to Y.S. from Lund University. We also thank Mats Hansson for fruitful discussions.

[1] L. R. Milgrom, *The Colours of Life*, Oxford University Press, Oxford, **1997**.
[2] D. K. Lavallee, *Coord. Chem. Rev.* **1985**, *61*, 55–96.
[3] S. J. Baum, R. A. Plane, *J. Am. Chem. Soc.* **1966**, *88*, 910–913.
[4] C. J. Walker, R. D. Willows, *Biochem. J.* **1997**, *327*, 321–333.
[5] H. L. Shubert, E. Raux, K. S. Wilson, M. J. Warren, *Biochemistry* **1999**, *38*, 10660–10669.
[6] E. Raux, H. L. Schubert, M. J. Warren, *Cell. Mol. Life Sci.* **2000**, *57*, 1880–1893.
[7] C.-K. Wu, H. A. Dailey, J. P. Rose, A. Burden, V. M. Sellers, B.-C. Wang, *Nat. Struct. Biol.* **2001**, *8*, 156–160.
[8] S. Al-Karadaghi, M. Hansson, S. Nikonov, B. Jonsson, L. Hederstedt, *Structure* **1997**, *5*, 1501–1510.
[9] H. L. Schubert, E. Raux, A. A. Brindley, H. K. Leech, K. S. Wilson, C. P. Hill, M. J. Warren, *EMBO J.* **2002**, *21*, 2068–2075.
[10] M. Inamo, N. Kamiya, Y. Inada, M. Nomura, S. Funahashi, *Inorg. Chem.* **2001**, *40*, 5636–5644.
[11] P. Hambright in *Dynamic Coordination Chemistry of Metalloporphyrins* (Ed.: K. Smith), Elsevier, Amsterdam, **1975**, pp. 233–278.
[12] P. Hambright, *J. Am. Chem. Soc.* **1974**, *96*, 3123–3131.
[13] D. K. Lavallee in *Molecular Structure and Energetics, Vol. 9: Mechanistic Principles of Enzymatic Activity* (Eds.: J. F. Liebmann, A. Greenberg), VCH, New York, **1988**, pp. 279–314.
[14] S. Funahashi, Y. Inada, M. Inamo, *Anal. Sci.* **2001**, *17*, 917–927.
[15] M. J. Bain-Ackerman, D. K. Lavallee, *Inorg. Chem.* **1979**, *18*, 3358–3364.
[16] R. Åkesson, L. G. M. Pettersson, M. Sandström, U. Wahlgren, *J. Am. Chem. Soc.* **1994**, *116*, 8705–8713.
[17] F. P. Rotzinger, *J. Am. Chem. Soc.* **1996**, *118*, 6760–6766.
[18] L. Helm, A. E. Merbach, *Coord. Chem. Rev.* **1999**, *187*, 151–181.
[19] F. P. Rotzinger, *J. Am. Chem. Soc.* **1997**, *119*, 5230–5238.
[20] P. E. M. Siegbahn, M. R. A. Blomberg, *Annu. Rev. Phys. Chem.* **1999**, *50*, 221–249.
[21] P. E. M. Siegbahn, M. R. A. Blomberg, *Chem. Rev.* **2000**, *100*, 421–437.
[22] C. Rovira, K. Kunc, J. Hutter, P. Ballone, M. Parrinello, *J. Phys. Chem. A* **1997**, *101*, 8914–8925.
[23] T. G. Spiro, P. M. Kozlowski, *Acc. Chem. Res.* **2001**, *34*, 137–144.
[24] E. Sigfridsson, U. Ryde, *J. Inorg. Biochem.* **2002**, *91*, 116–124.
[25] T. Andruniow, M. Z. Zgierski, P. M. Kozlowski, *J. Phys. Chem. B* **2000**, *104*, 10921–10927.
[26] N. Dölker, F. Maseras, A. Lledos, *J. Phys. Chem. B* **2001**, *105*, 7564–7571.
[27] K. P. Jensen, U. Ryde, *J. Mol. Struct. (THEOCHEM)* **2002**, *585*, 239–255.
[28] A. Ghosh, T. Wondimagegn, H. Ryeng, *Curr. Opin. Chem. Biol.* **2001**, *5*, 744–750.
[29] E. Sigfridsson, U. Ryde, *J. Biol. Inorg. Chem.* **2003**, *8*, 273–282.
[30] A. A. Jarzecki, P. M. Kozlowski, P. Pulay, B.-H. Ye, X.-Y. Li, *Spectrochim. Acta Part A* **1997**, *53*, 1195–1209.
[31] P. M. Kozlowski, T. G. Spiro, A. Bérces, M. Z. Zgierski, *J. Phys. Chem. B* **1998**, *102*, 2603–2608.
[32] P. M. Kozlowski, T. G. Spiro, A. Bérces, M. Z. Zgierski, *J. Phys. Chem. B* **2000**, *104*, 10659–10666.
[33] P. Rydberg, E. Sigfridsson, U. Ryde, *J. Biol. Inorg. Chem.* **2004**, *9*, 203–223.
[34] E. B. Fleischer, J. H. Wang, *J. Am. Chem. Soc.* **1960**, *82*, 3498–3502.
[35] J. P. Macquet, T. Theophanides, *Can. J. Chem.* **1973**, *51*, 219–226.
[36] K. Letts, R. A. Mackay, *Inorg. Chem.* **1975**, *14*, 2993–2998.
[37] E. B. Fleischer, F. Dixon, *Bioinorg. Chem.* **1977**, *7*, 129–139.

[38] C. H. Tsai, J. Y. Tung, J. H. Chen, F. L. Liao, S. L. Wang, S. S. Wang, L. P. Hwang, C. B. Chen, *Polyhedron* **2000**, *19*, 633–639.
[39] T. P. G. Sutter, P. Hambright, *Inorg. Chem.* **1992**, *31*, 5089–5093.
[40] Y. Inada, Y. Sugimoto, Y. Nakano, S. Funahashi, *Chem. Lett.* **1996**, 881–882.
[41] Y. Inada, Y. Sugimoto, Y. Nakano, Y. Itoh, S. Funahashi, *Inorg. Chem.* **1998**, *37*, 5519–5526.
[42] Y. Inada, Y. Nakano, M. Inamo, M. Nomura, S. Funahashi, *Inorg. Chem.* **2001**, *40*, 4793–4801.
[43] Y. Shen, U. Ryde, *J. Inorg. Biochem.* **2004**, *98*, 878–895.
[44] D. Lecerof, M. N. Fodje, A. Hansson, M. Hansson, S. Al-Karadaghi, *J. Mol. Biol.* **2000**, *297*, 221–232.
[45] M. P. Roach, S.-I. Ozaki, Y. Watanabe, *Biochemistry* **2000**, *39*, 1446–1454.
[46] R. F. Pasternack, N. Suting, D. H. Turner, *J. Am. Chem. Soc.* **1976**, *98*, 1908–1913.
[47] D. Lecerof, M. M. Fodje, R. A. León, U. Olsson, A. Hansson, E. Sigfridsson, U. Ryde, M. Hansson, S. Al-Karadaghi, *J. Biol. Inorg. Chem.* **2003**, *8*, 452–458.
[48] V. M. Sellers, C.-K. Wu, T. A. Dailey, H. A. Dailey, *Biochemistry* **2001**, *40*, 9821–9827.
[49] A. D. Becke, *Phys. Rev. A* **1988**, *38*, 3098–3100.
[50] J. P. Perdew, *Phys. Rev. B* **1986**, *33*, 8822–8824.
[51] A. Schäfer, C. Huber, R. Ahlrichs, *J. Chem. Phys.* **1994**, *100*, 5829–5835.
[52] A. Schäfer, H. Horn, and R. Alrichs, *J. Chem. Phys.* **1992**, *97*, 2571–2577.
[53] K. Eichkorn, O. Treutler, H. Öhm, M. Häser, R. Ahlrichs, *Chem. Phys. Lett.* **1995**, *240*, 283–290.
[54] K. Eichkorn, F. Weigend, O. Treutler, R. Ahlrichs, *Theor. Chem. Acc.* **1997**, *97*, 119–124.
[55] R. H. Hertwig, W. Koch, *Chem. Phys. Lett.* **1997**, *268*, 345.
[56] E. Sigfridsson, M. H. M. Olsson, U. Ryde, *J. Phys. Chem. B* **2001**, *105*, 5546–5552.
[57] M. H. M. Olsson, U. Ryde, *J. Am. Chem. Soc.* **2001**, *123*, 7866–7876.
[58] U. Ryde, K. Nilsson, *J. Am. Chem. Soc.* **2003**, *125*, 14232–14233.
[59] C. W. Bauschlicher, *Chem. Phys. Lett.* **1995**, *246*, 40.
[60] U. Ryde, M. H. M. Olsson, *Int. J. Quantum Chem.* **2001**, *81*, 335–347.
[61] A. Klamt, J. Schüürmann, *J. Chem. Soc. Perkin Trans. 2* **1993**, 799–805.
[62] A. Schäfer, A. Klamt, D. Sattel, J. C. W. Lohrenz, F. Eckert, *Phys. Chem. Chem. Phys.* **2000**, *2*, 2187–2193.
[63] A. Klamt, V. Jonas, T. Bürger, J. C. W. Lohrenz, *J. Phys. Chem. A* **1998**, *102*, 5074–5085.
[64] F. Jensen, *Introduction to Computational Chemistry*, Wiley, **1999**.
[65] Gaussian 98 (Revision A.9), M. J. Frisch, G. W. Trucks, H. B. Schlegel, G. E. Scuseria, M. A. Robb, J. R. Cheeseman, V. G. Zakrzewski, J. A. Montgomery, R. E. Stratmann, J. C. Burant, S. Dapprich, J. M. Millam, A. D. Daniels, K. N. Kudin, M. C. Strain, O. Farkas, J. Tomasi, V. Barone, M. Cossi, R. Cammi, B. Mennucci, C. Pomelli, C. Adamo, S. Clifford, J. Ochterski, G. A. Petersson, P. Y. Ayala, Q. Cui, K. Morokuma, D. K. Malick, A. D. Rabuck, K. Raghavachari, J. B. Foresman, J. Cioslowski, J. V. Ortiz, B. B. Stefanov, G. Liu, A. Liashenko, P. Piskorz, I. Komaromi, R. Gomperts, R. L. Martin, D. J. Fox, T. Keith, M. A. Al-Laham, C. Y. Peng, A. Nanayakkara, C. Gonzalez, M. Challacombe, P. M. W. Gill, B. G. Johnson, W. Chen, M. W. Wong, J. L. Andres, M. Head-Gordon, E. S. Replogle, J. A. Pople, Gaussian, Inc., Pittsburgh, PA, **1998**..
[66] R. Alrichs, M. Bär, M. Häser, H. Horn, C. Kölmel, *Chem. Phys. Lett.* **1989**, *162*, 165–169.

Received: March 26, 2004
Published online: January 20, 2005